carolinea, 63 (2005): 5-28, 11 Abb.; Karlsruhe, 15.03.2006

An Elasmosaur (Reptilia: Sauropterygia) from the Turonian (Upper Cretaceous) of Morocco

MARIE-CÉLINE BUCHY

Abstract

The subcomplete skeleton of an elasmosaurid plesiosaur recently acquired by the Staatliches Museum für Naturkunde Karlsruhe (State Museum of Natural History in Karlsruhe) is described. The specimen comes from the early Turonian of the Goulmima region, Morocco, and represents one of the most complete elasmosaurs known in the world. Owing to the present uncertainties about elasmosaurs systematics, it is referred mainly on stratigraphical grounds to a new species of the genus *Libonectes*. Some of the bones of the holotype (e.g. cervical vertebrae, ulna) show an unusual type of preservation that might indicate an old-age related pathology. Some aspects of elasmosaurs anatomy suggest non obligatory feeding upon sea floor invertebrates.

Kurzfassung

Ein Elasmosaurier (Reptilia: Sauropterygia) aus dem Turon (Oberkreide) von Marocco

Das fast vollständige Skelett eines elasmosauriden Plesiosauriers, welches kürzlich vom Staatlichen Museum für Naturkunde Karlsruhe erworben wurde, wird beschrieben. Das Stück stammt aus dem frühen Turon der Goulmima-Region Marokkos und ist eines der vollständigsten Elamosauridenskelette der Welt. Wegen der gegenwärtigen Unklarheiten in der Elasmosauriersystematik wird das Stück hauptsächlich aus stratigrafischen Gründen einer neuen Art der Gattung *Libonectes* zugeordnet. Einigen Knochen des Holotyps (z.B. Halswirbel, Ulna) zeigen eine ungewöhnliche Art der Erhaltung, welche auf alterspathologische Ursachen hindeutet. Einige Aspekte der Elasmosaurieranatomie legen die Möglichkeit nahe, dass die Tiere gelegentlich Meeresbodeninvertebraten gefressen haben.

Résumé

Un Élasmosaure (Reptilia: Sauropterygia) du Turonien (Crétacé supérieur) du Marocco

Le squelette subcomplet d'un plésiosaure élasmosauride récemment acquis par le Staatliches Museum für Naturkunde Karlsruhe (Muséum d'Histoire Naturelle de Karlsruhe) est décrit. Le spécimen provient du Turonien inférieur de la région de Goulmima, Maroc, et représente l'un des élasmosaures les plus complets au monde. En raison des incertitudes entourant à ce jour la systématique des élasmosaures, il est attribué, surtout sur des arguments stratigraphiques, à une nouvelle espèce du genre *Libonectes*. Certains des os de l'holotype (par exemple des vertèbres cervicales, l'ulna) présentent un type de préservation inhabituel qui pourraient indiquer une pathologie liée à un âge avancé. Certains aspects de l'anatomie des élasmosaures suggèrent qu'ils s'alimentaient partiellement aux dépends des invertébrés du fond marin.

Autor

MARIE-CÉLINE BUCHY, Universität Karlsruhe, Geologisches Institut, Postfach 6980, D-76128 Karlsruhe, Germany. Current address: Geowissenschaftliche Abteilung, Staatliches Museum für Naturkunde, Erbprinzenstrasse 13, D-76133 Karlsruhe, Germany; mcbuchy@myway.com

Introduction

Elasmosaurs form a family of plesiosaurs characterised by an elongate neck bearing a small, brevirostrine head. Elongation of the neck is achieved by both elongation of the vertebrae and increase in vertebral count. They appear in the fossil record during the Early Jurassic of Europe and are known world-wide by the Late Cretaceous (PERSSON 1963, BARDET 1995, BARDET et al. 1999, LAZO & CICHOWOLSKI 2003), though they are most abundant in the Upper Cretaceous sediments of North America (e.g. WILLISTON 1890, 1906, WELLES 1962, CARPENTER 1999, STORRS 1999, GASPARINI et al. 2003, EVERHART in press). The record of elasmosaurs from Africa is limited to fragmentary remains (for a review see WERNER & BARDET 1996) and some unspecified remains from the area of Goulmima, Morocco (BARDET et al. 2000, BARDET pers. comm.).

Goulmina has yielded a rich fish assemblage (CAVIN 1995, 1997, 1999, 2001, CAVIN et al. 2001) and marine reptiles (BARDET et al. 2003a, b). Most described specimens were acquired via fossil dealers, their exact origin being unknown. Several workers undertook field work in order to define the provenance of the vertebrate-bearing nodules (CAVIN 1999, CAVIN et al. 2001, BARDET et al. 2003a) and concluded that the nodules occur at the top of the Cenomanian-Turonian section, in the Unit 4 defined by FERRANDINI et al. (1985). This unit is dated by the ammonite *Mammites* to the early Turonian and was deposited under open platform conditions at the maximum of the Cenomanian-Turonian transgression (FERRANDINI et al. 1985, CAVIN 1999, BARDET et al. 2003a). Marine reptiles from Goulmima include mosasaurs and plesiosaurs (BARDET et al. 2000, 2003a, b, BUCHY et al. 2005, BARDET pers. comm.). The specimen herein described is the first diagnostic elasmosaur of the assemblage, and one of the most complete and best preserved elasmosaurs known in the world.

Institutional abbreviations

ANSP: Academy of Natural Sciences, Philadelphia, USA; AMNH: American Museum of Natural History, New York, USA; CIT: California Institute of Technology, Pasadena, USA; DMNH: Denver Museum of Natural History, Denver, USA; FMNH: Field Museum for Natural History, Chicago, USA; KUVP: Kansas University, Vertebrate Paleontology, Museum of Natural History, Lawrence, USA; MSGB: Museo del Servicio Geológico, Bogotá, Colombia; NZGS: New zealand Geological Sruvey, Lower Hutt, New Zealand; RSM: Royal Saskatchewan Museum, Regina, Canada; SMNK: Staatliches Museum für Naturkunde Karlsruhe; SMNS: Staatliches Museum für Naturkunde Stuttgart; SMUSMP: Southern Methodist University, Shuler Museum of Natural History, Dallas, USA; UCMP: University of California Museum of Paleontology, Berkeley, USA; UNSM: University of Nebraska State Museum, Lincoln, USA.

Material and Preservation

The specimen (Plate 1, Figs 1-9) was obtained via a fossil dealer in the autumn of 2002, together with the polycotylid plesiosaur SMNK-PAL 3861 (BUCHY et al. 2005); it is housed in the SMNK under accession number SMNK-PAL 3978. It consists in a subcomplete, articulated, 3-dimensionally preserved skeleton lacking parts of the left limbs and the terminal caudal vertebrae; both right limbs are missing except for the humerus and femur. The locality data associated with SMNK-PAL 3978 are the same as for SMNK-PAL 3861 (BUCHY et al. 2005): both come from ‘some kilometres around Goulmima’, Morocco. The calcareous matrix surrounding SMNK-PAL 3978 is similar to that surrounding SMNK-PAL 3861, which agrees with the vertebrate-bearing nodules known from the early Turonian of the Goulmima area (CAVIN 1995, 1997, 1999, 2001, CAVIN et al. 2001, BARDET et al. 2003a, b, BUCHY et al. 2005, BARDET pers. comm.). The presence of the ammonite *Fagesia superstes* (KOSSMAT, 1897) preserved with SMNK-PAL 3978 confirms the late early Turonian to early middle Turonian age of the fossil (CHANCELLOR et al. 1994, C. IFRIM pers. comm.).

The specimen is currently on exhibition at the SMNK, resting on its ventral side (Plate 1). Most elements of the girdles are therefore inaccessible for study. The length of the skeleton as preserved is about 7.2 m. Mechanical preparation was completed prior to purchase by the SMNK. For the non-preserved right limb elements distal to the propodials, casts of the left ones were substituted (Plate 1). The left forelimb is mostly genuine (Fig. 8), although the distal-most portion probably belongs to another limb (see Description). The fifth metatarsal (e.g. WELLES 1943, CALDWELL 1997, SATO 2003) situated cranially indicates that the hindlimb placed on the left side of the specimen is either visible in ventral aspect or is actually the right one (Fig. 9). The proximal two thirds of this hindlimb are genuine; its distal third is a cast of the distal extremity of the left forelimb (see Description). Except for a few aesthetic patches of coloured resin, mainly in the skull and mandible (Figs 1, 2, 4), the rest of the skeleton appears genuine.

All preserved neural arches are fused, indicating an adult individual *sensu* BROWN (1981).

Numerous cervical vertebrae of the caudal three-fourths of the neck, some ribs and long bones (Figs 7-9, Table 1) are incompletely preserved. When the affected element is not distorted, a brownish area that contrasts with the surrounding light beige matrix replaces the missing bone substance as if it were a natural cast. The darker brown edge of the damaged bone, where exposed, has a finished, smooth aspect. Other elements are distorted as if they were soft in places when diagenesis occurred, e.g. cervicals wedged between adjacent cervicals, without broken bone fragments (Fig. 7). This uncommon preservation is interpreted as due to a probable pathology that might indicate an old adult (see Discussion).

Systematic Palaeontology

Sauropterygia OWEN, 1860
Plesiosauria DE BLAINVILLE, 1835
Plesiosauroidea WELLES, 1943
Elasmosauridae COPE, 1869
Libonectes CARPENTER, 1997
Libonectes atlasense n. sp.

Holotype – SMNK-PAL 3978, skeleton lacking both right limbs distal to the propodials, parts of the left limbs and the terminal caudal vertebrae (Plate 1, Figs 1-9).

Type horizon and locality – Lower Turonian (Upper Cretaceous) Unit 4 of the Cenomanian-Turonian limestone bar, north of Goulmima, Errachidia Province, Morocco (FERRANDINI et al. 1985; CAVIN 1999: fig. A; BARDET et al. 2003a: fig. 1).

Etymology – Latin, from the north African Atlas (Mountain Range).

Diagnosis – An elasmosaur differing from the type specimen of *Libonectes* (CARPENTER 1997, 1999) in the following features: The ventral margin of the upper cheek is concave between premaxillary tooth 3 and maxillary tooth 3 on the right side, and 5 on the left. The naris is situated level with maxillary teeth 4-5, which are the largest teeth in the upper tooth row. The mandibular rostrum comprises 3 teeth; a ventrocaudally oriented, flat chin extends until level with the rostral end of the maxilla. 52-53 cervical and 5-7 pectoral vertebrae. The axis neural arch is 1.5 time higher than its centrum; the axis postzygapophysis entirely overhangs the centrum of the third cervical.

Referred specimen – SMNS 81783, poorly preserved skull and mandible (Fig. 10), from the same locality and age as the holotype.

Description

Axial skeleton

Skull (Figs 1, 2, 4, 5)

The skull is typically elasmosaurian, comprising a preorbital section (about 38% of skull length) slightly shorter than the postorbital section, which is distinguished by a high parietal crest.

Table 1. Bones of SMNK-PAL 3978 probably affected by a pathological decrease in bone density; location of the lesions. Most of the girdles and dorsal vertebrae being obscured by matrix or currently inaccessible, the list is not exhaustive. Lesions preceded by an asterisk are not clearly visible but suspected because of important distortion of the bone that cannot be explained by diagenesis (see Preservation and e.g. Fig. 7).

Bone	Place of lesion
left humerus	*linear, at the distal extremity of the shaft, transverse to the shaft
left ulna	linear, in the middle of the shaft, transverse to the shaft
left femur	ventral half proximal to at least mid shaft
right femur	cranioproximal portion until at least mid shaft
‚right‘ tibia	*linear, in the middle of the shaft, transverse to the shaft
‚right‘ fibula	*linear, in the middle of the shaft, transverse to the shaft
C15	left dorsocaudal corner of centrum and base of neural spine
C16	caudal articular margin of centrum
C17	*oblique line ventrocaudally directed through centrum
C23	*ventrocaudal corner of centrum
C24	*caudal articular margin of centrum
C26	*middle of centrum
C28	caudal articular margin of centrum and left pedicel
C29	dorsocaudal corner of centrum and neural arch in continuity (except caudal margin of the arch)
C30	*cranioventral margin of left rib
C32	caudal articular margin of centrum
C33	cranial articular margin of centrum
C34	dorsal portion of caudal articular margin of centrum
C35	*rectangular lesion in left dorsocaudal corner of centrum
C36	*centrum
C38	*centrum
C39	cranial articular margin of centrum
C40	cranial articular margin of centrum and cranial portion of neural arch
C41	*right dorsocaudal corner of centrum
C42	*right side of centrum and neural arch
C46	middle of caudal left articular margin of centrum
C47	cranial articular margin of centrum
C48	caudal articular margin of centrum
C51	cranial articular margin of centrum
C57	base of left neural arch
right rib 63	in the broken area (see text)
right rib 64	transverse area 20 mm proximal to articular head

The skull is ogival in dorsal aspect, and triangular in lateral aspect (Figs 1, 2). WILLISTON (1890) and numerous others since (e.g. WELLES 1952, CARPENTER 1999, SATO 2003) complained of the poor preservation of sutures and osteological details in most elasmosaurian skulls. SMNK-PAL 3978 is no exception. Although the skull is only slightly sheared rightward (Fig. 4), it is impossible to determine the course of many of the sutures due to numerous breaks. This is especially the case in the interorbital area, where no individual bone can be distinguished with certainty, and no suture distinguished from breaks (Figs 2, 4). The lateral shear caused breakage to the dorsolateral portions of the squamosal in a symmetrical manner (Figs 1, 2); this breakage pattern, known in several specimens, led some authors to suggest the presence of a quadratojugal (WILLISTON 1890, WELLES 1943, 1949, 1952, 1962). However, no quadratojugal is nowadays considered existing in plesiosaurs (e.g. WILLISTON 1925, ROMER 1956, BROWN 1981, STORRS 1997, CARPENTER 1997). Due to the same distortion, the suspensorium of SMNK-PAL 3978 is inclined rostroventrally (Fig. 1); given the general pattern of deformation, that affected the skull in a dorsoventral and rightward direction (see Fig. 4), it was probably subvertical *in vivo*.

Owing to these uncertainties about the location of the sutures, the present description considers the skull as a whole instead of focusing on individual bones. Moreover, the skull appears very conservative in the group (CARPENTER 1999), and was described in detail by WILLISTON (1890), WELLES (1943) and CARPENTER (1997) among others; therefore only features specific to SMNK-PAL 3978 are treated here. Measurements on the skull and mandible are given in Table 2.

Table 2. Measurements in mm of the skull and mandible of SMNK-PAL 3978. Definition of the measurements was discussed by BUCHY et al. (2005: Appendix); here, owing to the lateral distortion of the skull, the skull length is measured between the rostral extremity of the skull and the caudal-most margin of the quadrate condyle.

skull length	400
temporal fenestra length	165
orbit maximal diameter	57
preorbital length	155
skull width	185
interorbital minimal width	60
mandible length	450
mandibular symphysis length	40
maximal visible length of the dentary tooth row	270

The left premaxilla houses 4 teeth, the right one 5. The premaxillomaxillary suture commences at the rostral-most point of the naris; it smoothly curves laterally and ventrally (Figs 1, 2). On both sides, its ventral-most extent is obscured by the third visible dentary tooth and adjacent matrix. Two ridges parallel the interpremaxillary suture (the dorsal midline) on the surface of the left premaxilla for about half the rostrum length. The premaxilla forms the medial margin of the naris, but the extent of the bone in the interorbital area cannot be determined. The ventral margin of the right upper jaw is concave from premaxillary tooth 3 to maxillary tooth 3. The ventral concavity of the left upper jaw extends from premaxillary tooth 3 to maxillary tooth 5. On both sides, the ventral margin of the upper jaw is obscured by matrix caudal to the rostral margin of the orbit, that is, caudal to maxillary tooth 9 (Fig. 5).

The right naris is oval in dorsal aspect, its long axis oriented rostrolaterally; the original outline of the left one cannot be determined. Both are situated level with maxillary teeth 4-5. On the left side, the 7 rostral-most maxillary teeth alternate with dentary teeth; another maxillary tooth is visible ventral to the orbit; all other left maxillary teeth are obscured by matrix and dentary teeth. Similarly, on the right, 6 maxillary teeth alternate with dentary teeth, and a further maxillary tooth is visible ventral to the orbit. The maxilla appears to form most of the lateral margin of the naris; the caudal margin of the naris is formed by the prefrontal. Though, the suture between the maxilla and prefrontal is only visible on the left, where the outline of the naris is unclear. The maxilloprefrontal suture runs to the rostral margin of the orbit, whose rostrolateral corner is formed by the maxilla. The jugal appears to form most of the ventral margin of the orbit; the suture of this bone with the maxilla runs caudoventrally but is soon obscured by teeth and matrix. The rostromedial margin of the orbit is formed by the prefrontal. The medial margin of this bone runs from the caudal-most point of the naris to the centre of the medial margin of the orbit.

A break affecting the centre of the right postorbital bar, and a similar, symmetrical structure on the left side probably occurred at the medial margins of the postorbitals, which, I conclude, form the caudal margins of the orbits. The lateral margin of the postorbital (its suture with the jugal) runs caudally from the caudoventral corner of the left orbit in lateral aspect, sigmoidal; it is preserved for about 30 mm. The temporal bar is broken in its middle on both sides; it is unclear whether this break can be interpreted as the caudal extremity of the jugal.

The parietal crest is parallel-sided in dorsal aspect, and partly reconstructed; no parietal foramen is visible, although it might not be identifiable in the caudal portion of the poorly preserved interorbital area. The caudal extent of the parietal and its suture with the squamosal cannot be determined. The contact between quadrate and squamosal is also invisible. As preserved, the caudal part of the skull is boomerang-shaped in dorsal aspect.

Mandible (Figs 1, 3-5)

The mandibular rostrum houses 3 tooth positions. The mandibular symphysis commences level with left premaxillary tooth 4. In ventral aspect, it is visible running straight rostrally for about 20 mm. It cannot be traced further rostrally. From the rostral extremity of the visible portion of the symphysis a ridge diverges rostrolaterally on either side. The triangular area between these ridges is flat. In lateral aspect the rostral margin of the mandible is straight, caudoventrally oriented, and persists so until level with the rostral-most extent of the maxilla. The ventral margin of the mandible caudal to this point is straight, horizontal. The dorsal margin of the lower jaw is slightly concave until about the level of the rostral margin of the supratemporal fenestra; it is horizontal further caudally. Seventeen dentary teeth are visible on the left, 16 on the right plus one empty alveolus (Table 3). The dentary is the only visible bone in lateral aspect until level with the middle of the temporal bar. There, a vertical break is continuous with the break affecting the temporal bar; the caudal extent of the dentary cannot be determined. The angulosurangular suture emerges caudal to this break at mid-height on the mandible and runs caudally; the dorsal margin of the angular then outlines the glenoid fossa. The dorsal margin of the angular cannot be traced further caudally on the lateral surface of the retroarticular process. The rostral margin of the articular (its suture with the surangular) is not identifiable. The retroarticular process extends caudally until level with the centre of cervical vertebra 3.

Dentition (Figs 1-5)

The enamel is damaged on several teeth. Most of the largest teeth of the right row were recently broken. Otherwise the teeth are well preserved, but only visible in labial view. Basal diameter and height of the teeth when determinable are given in Table 3. The tooth count, occlusion pattern and location of the naris and orbit compared to maxillary and dentary teeth are shown in Figure 5.

The rostral-most premaxillary tooth pair is strongly procumbent. The second premaxillary tooth pair is curved and points rostroventrally; successive upper teeth become progressively more vertical. The dentary teeth are more uniform in

Table 3. Basal diameter and height in mm of the tooth crowns of SMNK-PAL 3978. Italicised values are estimate; crowns whose height is in brackets are recently broken, while the sign '+' following crown height indicates a naturally worn apex.

Left tooth no	Basal diameter	Height	Right tooth no	Basal diameter	Height
pmx 1	*5*	17	pmx1	6	21
2	10	30+	2	*6*	(17)
3	*9*	25+	3	*7*	(13)
4	9	33+	4	*9*	(21)
			5	8	(14)
mx 1	7	15+	mx 1	*5*	(17)
2	7	24+	2	4	15+
3	*7*	(20)	3	7	(10)
4	11	41+	4	7	13+
5	10	39+	5	8	23+
6	6	27+	6	*5*	(16)
7	4	(10)	7	*5*	13+
8	/	(10)	8	*3*	(10)
d 1	*8*	27+	d 1	7	(24)
2	10	33 +	2	6	25+
3	*10*	34+	3	*6*	30+
4	3	(10)	4	*5*	21+
5	9	(27)	5	*6*	(31)
6	2	(7)	6	8	30+
7	7	17+	7	6	20+
8	/	/	8	6	(24)
9	8	30+	9	*6*	28
10	7	28+	10	7	28
11	7	29	11	7	22+
12	7	23	12	7	27+
13	6	14	13	/	/
14	8	22+	14	8	30+
15	6	13	15	7	22
16	7	20+	16	8	30+
17	*3*	*6*	17	*7*	/

orientation; all point vertically and are slightly curved.

The enamel exhibits faint striae toward the base of the crowns on the labial face. All tooth crowns are subcircular to weakly oval in basal cross-section; no carina is visible. Right premaxillary tooth crowns 1 and 5, maxillary crown 5, dentary crowns 10 and 12, and possibly left maxillary crown 5 exhibit a basal band of wrinkled enamel, 1-2 mm in thickness, presumably all around the crown base. This might mark a growth abnormality, maybe due to a deficiency; further preparation could clarify whether it actually occurs mostly on the right side and help establish a diagnosis. Most apices were either broken recently or worn *in vivo* (Table 3); the intact ones are rounded instead of sharp and taper abruptly.

Vertebrae and ribs (Figs 6, 7)

The atlas/axis complex is preserved close to its original position, but due to incomplete preparation only its caudal portion is visible. On the right side, the base of both neural arches, part of the odontoid, and most of the axis and its cervical rib are exposed, the bone surface being poorly preserved. On the left, the axis neural arch and centrum and the proximal-most portion of the cervical rib are visible (Fig. 6). The distal-most portion of the atlas neural arch appears to contact the axis neural arch dorsocaudal to the zygapophyseal contact; adhering matrix, though, renders interpretation problematic. The suture of the atlas neural arch with the odontoid as visible on the right is almost straight and runs slightly cranioventrally, forming a ridge; the suture between the axis neural arch and its centrum extends caudally from the caudal-most point of the suture of the atlas neural arch with the odontoid. The axis neural arch extends caudally over the cranial half of cervical centrum 3; the postzygapophysis projects entirely caudal to the axis centrum. The axis neural arch is 1.5 time higher than its centrum. A conspicuous, rounded ridge runs parallel to the dorsal margin of the neural arch at mid-height. The right axis rib smoothly curves distocaudally; it tapers distally and its distal terminus is rounded.

Together with the atlas and axis, the neck comprises at least 52 cervical vertebrae; vertebra 53 is too poorly preserved to determine whether it is a cervical or a pectoral. Vertebra 54 is a pectoral and so are the following 5 vertebrae. The 60th vertebra of the series is either the last pectoral or first dorsal, but the insertion area of the transverse process cannot be defined. The length of the cervicals and pectorals, where determinable, is given in Table 4. On the right side, a ridge is preserved at mid-height on the centra until C39; on the left until C48 (the ridge is less expressed from C42 to C48). The cross-sectional shape of the vertebrae is unclear, as most breaks pass through vertebrae rather than between them. Where visible, the centra are weakly dorsoventrally compressed in cross-section (Fig. 7). A centrimetric intervertebral space is preserved until between C39 and C40, and probably between C40 and C41; further caudally, the articular surfaces of subsequent vertebrae as preserved appear separated by only a few millimetres. From C4, half the length of the postzygapophysis of each vertebra projects over the cranial margin of the succeeding centrum. Until C16 the neural spines are inclined caudally at an angle of 45° to the horizontal. Further caudally, the neural spines seem to point vertically, but are only completely preserved between C39 and C41. The neural spines of C41 to C43 are fan-shaped distally; whether this represents their original shape or is due e.g. to pathology or diagenesis is unknown.

All cervical ribs are fused to the centra; the suture line is visible as a swollen line on C5 to C7 The third cervical rib is subtriangular in lateral aspect. Its distal extremity tapers caudally and reaches a level 10 mm caudal to the cranial margin of the

Table 4. Length in mm of the cervical and pectoral corpora of SMNK-PAL 3978. Italicised values are estimate.

No.	Length (mm)	No.	Length (mm)	No.	Length (mm)
atax	/	C21	80	C40	*90*
C3	34	C22	69	C41	*100*
C4	*35*	C23	75	C42	95
C5	34	C24	66	C43	85
C6	32	C25	*65*	C44	90
C7	*40*	C26	/	C45	*95*
C8	38	C27	/	C46	95
C9	*40*	C28	*80*	C47	*97*
C10	42	C29	*72*	C48	80
C11	*45*	C30	79	C49	87
C12	55	C31	*75*	C50	*82*
C13	55	C32	*80*	C51	*83*
C14	60	C33	*80*	C52	*65*
C15	69	C34	78	C53	*79*
C16	*60*	C35	72	P1	69
C17	*70*	C36	*80*	P2	68
C18	66	C37	*80*	P3	73
C19	65	C38	*78*	P4	80
C20	*70*	C39	90	P5	*80*

centrum of C4. A break runs through C4, obscuring the shape of the associated ribs. Between C5 and C46, the shaft of each rib is nearly vertical, and its distal extremity is expanded cranially and caudally, being thus hammer-shaped. Further caudally, the cervical ribs taper distally. Each rib is longer than the height of the respective centrum on C4 to C10; the ribs are as long as the centra are high on C11 to C18, and shorter than the height of the centra between C19 and C50. The ribs then become progressively longer toward the thorax. Except maybe the third pair, all ribs are laterally convex. They insert on the ventrolateral portion of the centra, slightly caudally, at least until C48. The pectoral ribs are only partly preserved; they were not fused to the transverse processes and, like the thoracic ribs, collapsed and now lie on their cranial face. The proximal portion of the shaft of the pectoral ribs exhibits a well-defined, caudally directed crest.

The dorsal vertebrae are hardly visible, due to matrix and ribs. In the cranial portion of the thorax, 10 are identified by their transverse processes. Toward the pelvic girdle, the column is disarticulated. Vertebrae 70 to 77 are lying on their right side, and their neural arches are separated from the respective centra; vertebra 75 partially overlaps vertebra 76, and a further vertebra might be present in the area. The first clear sacral vertebra, bearing a large, kidney-shaped rib facet in the centre of the lateral face of the centrum, is the 76th (or 77th) in the series. The following vertebra is also a sacral, while the 78th (or 79th) is too poorly preserved to determine whether it is a sacral or the first caudal. Where visible, the dorsal and sacral centra are cylindrical, slightly higher than long; they appear to be in close contact with one another. The neural spines are missing on all dorsal vertebrae, broken at their base. On the right side, seven of the cranial-most thoracic ribs are largely preserved, collapsed like the pectoral ribs; like them, they were not fused to the transverse processes. The right ribs associated with vertebrae 60 to 63 had been broken at the level of the ventral curvature of the shaft, and calluses grew at the fractured area. The left ribs are missing, or are represented by disarticulated fragments.

Twelve caudals are partly preserved, although much of these is reconstructed, at least superficially. The centra are wider than long. All neural spines are missing. The poorly preserved transverse processes are horizontal, with parallel cranial and terminal margins.

The caudal-most median elements of the gastral basket are preserved in articulation between the vertebral column and left hindlimb. The gastralia exhibit the typical, spindle shape, with a shallow, longitudinal groove on their exposed surface.

Appendicular skeleton

Pectoral girdle

As the specimen is exposed, only isolated portions of the pectoral girdle are visible, so that no reliable interpretation can be given. The right pectoral fenestra is insufficiently exposed to determine whether a pectoral bar is present.

Pelvic girdle (Fig. 9)

The left pubis partly overlies the left femur. The cranial-most portion of its medial margin is in turn overlain by what is probably the same portion of the right pubis. Sacral ribs obscure the rest of the medial margin of the left pubis. The medial and cranial margins of the pubis appear to form an obtuse angle. The cranial margin runs straight craniolaterally, at least in its preserved, medial-most portion. The lateral margin is smoothly concave. The left pubis is still in natural contact with the laterocranial-most, acetabular portion of the ischium. The proximal portion of the ilium is probably represented by an enlarged acetabular head, smoothly curving into a parallel-sided shaft, preserved over about 70 mm.

Forelimb (Fig. 8)

The shaft of the left humerus is set off from its distal portion, both parts being separated by a break. It thus appears that the same disease as several vertebrae (see Material and Discussion; Table 1) and ulna (see below) affected the humerus at the distal end of its shaft; the humerus may have been compressed proximodistally when the carcass touched the sea floor, breakage occurring in the affected area. Comparison with the preserved portion of the right humerus appears to confirm that the left humerus was about one fourth longer than it is as preserved. The cranial margin of the humerus is only slightly concave in its proximal portion. In its distal third the cranial margin forms a distinct shoulder. The caudal margin of the humerus is smoothly concave. The distocaudal-most corner of the bone is missing. The articular facets for the radius and ulna are shallowly concave in dorsal aspect and subequal in length. The interarticular area is situated level with the centre of the shaft.

The radius is subquadrangular with a convex cranial margin and a concave caudal margin.

Only the distal portion of the ulna is preserved. A natural cast (see Material and Discussion) seemingly replaced the middle portion of its shaft; it appears that more of the bone was preserved proximally as its proximal edge consists of freshly broken bone. The cranial margin of the ulna as preserved is concave; its distal margin is divided into a cranial facet for the intermedium or centrale (see CALDWELL 1997, SATO 2003), a central, longer facet for the ulnare, and a third facet, slightly longer than the facet for the intermedium but incompletely preserved, for supernumerary bone(s).

The radiale is subrectangular with rounded angles and convex cranial and caudal margins. Its proximocranial corner forms a proximally directed hook. The intermedium is hexagonal. The ulnare is subquadrangular with rounded angles, a convex cranial margin and a concave caudal margin.

Identification of the elements of the distal carpal and tarsal rows in plesiosaurs was last discussed by SATO (2003); it appears reasonable to consider the second element as fused distal carpals (tarsals) 2 and 3, as they articulate with metacarpals (-tarsals) II and III. Distal carpals 1 and 2+3 are subquadrangular, the former one-third larger than the latter. Distal carpal 4 is subrectangular, craniocaudally elongate. The caudal-most element of the carpal row is metacarpal V, which is typically hour-glass-shaped and proximodistally elongate; it is incompletely exposed proximally.

Metacarpals I-III are entirely preserved; they are hour-glass-shaped as are the phalanges. Only the proximal-most portion of metacarpal IV is genuine.

In the stylopod, a break runs distal to phalanges I6, II5, III4, IV3 and ?V4 (see further). Proximal to this break, the phalanges of the first digit regularly decrease in size distally. Distal to the break, the phalanges forming the cranial-most digit are larger than the last phalanges of the proximal portion of digit I, thus casting a serious doubt about the origin of this genuine, distal fragment. It most likely does not belong where it is located, and digit I was probably the shortest digit of the forelimb, as is the case for all plesiosaurs known (e.g. CALDWELL 1997). It is unknown, where the distal fragment comes from. Therefore, 6 phalanges are surely preserved in digit I, 5 in digit II, and 4 in digit III. Of digit IV, bones are reconstructed between the metacarpal and the centre of the ?second phalanx; the third phalanx is genuine. The whole digit V is missing, except for the distal-most portion of what appears to be the fourth phalanx.

Hindlimb (Fig. 9)

At least proximal to mid-shaft, the ventral half of the left femur is entirely missing and was probably preserved as a cast (see Material and Discussion). The caudal margin of the left femur is smoothly concave. Due to the overlying pubis, only the straight articular facet for the fibula is visible. Taking into account the shortening of the left humerus, both propodials have about the same proximodistal dimension. The right femur preserves no further anatomical details, its visible, ?dorsal aspect being weathered and having been partly preserved as a cast.

As noted earlier (see Material), the portion of the hindlimb placed on the left side of the mounted specimen distal to the femur is either the right one or visible in ventral view. For the present description, the latter hypothesis is adopted; it appears to agree better with the loss, probably due to weathering, of the distal portions of both right limbs.

The middle portion of the tibia is reconstructed; it was probably preserved as a cast. The cranial margin of the tibia is convex, its caudal margin concave; its cranial corners are rounded while its caudal corners are pointed. Its proximal margin is convex cranially and concave caudally; its distal margin is weakly convex.

Less than the distal half of the fibula is genuine. The preserved portions of its cranial and caudal margins are parallel, craniodistally directed. Its distal margin is convex, poorly divided into two articular facets, for the calcaneum and astragalus (traditionally interpreted respectively as fibulare and intermedium and recently reassessed by CALDWELL [1997] and SATO [2003]).

The centrale (traditionally tibiale, CALDWELL 1997, SATO 2003) is subrectangular with rounded cranioproximal and caudoproximal corners and a concave cranial margin. The proximal margin of the astragalus is obscured by matrix; both its cranial and caudal margins are straight; its distal margin is concave cranially and convex caudally. The proximal margin of the calcaneum is obscured by matrix as well. The bone is enlarged distally, where its otherwise straight cranial and caudal margins diverge. Its distal margin is convex.

The first distal tarsal is trapezoidal, its longer margin being the proximal one. Its cranioproximal corner is overlain by the hooked-shaped, cranially directed cranioproximal corner of distal tarsal 2+3 (see above). Apart from this hook, distal tarsal 2+3 is subquadrangular. Distal tarsal 4 is subquadrangular, its proximal and distal margins slightly convex, its cranial and caudal margins slightly concave. Metatarsal V is hourglass-shaped and follows the distal tarsal row caudally.

A break filled with resin runs from the caudodistal corner of metatarsal I through the shaft of metatarsals II–IV and the proximal margin of phalanx V1. The metatarsals otherwise are genuine, hourglass-shaped, and of similar size.

The stylopod is broken and reconstructed further distally, between the phalanx I2 and the distal margin of V1. The distal third of the hindlimb is a cast of the forelimb (see above). Thus only the following bones are surely genuine: phalanx I1, the caudal half of phalanxes I3 and I4 and the proximocaudal corner of the phalanx I5; half of phalanxes II1 and II2, phalanx II3 and half of phalanxes II4; half of phalanx III1, phalanxes III2 and III3; most of phalanxes IV1, IV2 and IV3; phalanxes V1, V2 and half of phalanx V3.

Referred specimen (Fig. 10)

SMNS 81783 is a weathered skull. It exhibits all features observed in SMNK-PAL 3978 listed in the diagnosis; moreover, it confirms that the suspensorium is subvertical.

Discussion

Comparative palaeontology

Although elasmosaurids are among the most famous reptiles of the Mesozoic (e.g. SHULER 1950, TAYLOR 1997) and form an anatomically homogenous, well-defined group among Plesiosauria, there are few adequately described skulls (Table 5). Referral of partial and sometimes juvenile specimens, based on post-cranial features of poorly proved taxonomical import, has often added new portions of the skeleton or even skull to taxa established upon incomplete holotypes, potentially creating chimeras in great need of reassessment. In consequence, elasmosaur systematics is currently still mostly based on postcranial features, as they were established in the latest reviews of American taxa (WELLES 1943, 1952, 1962); taxonomy is in great need of a comprehensive revision taking into account ontogeny and individual variation. Long-awaited recent clarifications (STORRS 1999, CARPENTER 1997, 1999, GROSSMANN in prep.) mainly considered geographically or stratigraphically defined groups of taxa. As a result, most elasmosaurian genera currently considered valid are monospecific and often monotypic, many being defined on poorly diagnostic features or material (Table 5). A profound lack of understanding of the anatomy of elasmosaurs in an evolutionary perspective results, which is exemplified by the number and nature of characteristics considered reliable for diagnosing elasmosaurian genera (CARPENTER 1999): number of cervical vertebrae, structure of the atlas/axis complex, position of the naris compared to maxillary teeth, and, for some taxa, absence of a pectoral bar in adults. *Hydralmosaurus* WELLES, 1943 appears unique in the extension of the caudodistal margin of its humerus. Of these characteristics, the import of the number of cervical vertebrae on taxonomy should be thoroughly assessed in a group that is defined by the elongation of its neck, not only by elongation of individual vertebrae but also by increase in their number. Individual variation in the number of vertebrae, including cervicals, occasionally occur in mammals (e.g. ROUVIÈRE & DELMAS 1985, NICKEL et al. 2004); large-scale studies in Recent reptiles are missing that would help estimate individual variations and their magnitude. Additionally, few elasmosaurs are known with complete cervical column and material allowing independent taxonomical identification. Given the uncertainty concerning the tooth count when skull and mandibles are preserved in occlusion (e.g. CARPENTER 1997), the extent of the nares and their position relative to the maxillary teeth is usually difficult to determine precisely, their margins being broken and pressed inward. These features are frequently used as a means to quantify a subjective impression concerning the caudal retreat of the naris and skull proportions, which depends much upon the amount of distortion the skull underwent.

SMNK-PAL 3978 undoubtedly represents an elasmosaurid plesiosaur as defined, for instance, by BROWN (1993) and BARDET et al. (1999). With 58 to 60 cervicals and pectorals ('cervicals' *sensu* CARPENTER 1999), SMNK-PAL 3978 is similar to most Late Cretaceous elasmosaurs for which this figure is known with certainty (Table 5). It probably only clearly differs from *Elasmosaurus*, which has as many as 72 cervicals (COPE 1868, CARPENTER 1999).

The humerus of SMNK-PAL 3978 is incompletely preserved caudally; though, the central location of the transitional area between the facets for

Table 5. Late Cretaceous elasmosaurs of import for comparison with SMNK-PAL 3978. The first cited specimen is the holotype of the taxon. The number of cervicals includes pectorals (for comparison with CARPENTER 1999) when not otherwise stated and is given for the holotype if not otherwise stated.

Taxon	Additional reference(s)	Material	Occurrence	Number of cervical vertebrae	Skull length (mm)
Callawayasaurus colombiensis (WELLES, 1962)	CARPENTER 1999	UCMP 38349, referred MSGB, subcomplete skeletons	Upper Apt Colombia	56	350 (holotype)
Aphrosaurus furlongi WELLES, 1943	WELLES 1952	CIT 2748, vertebrae, limbs and girdles; juvenile referred, skull fragments, vertebrae, partial pelvic girdle and limb	Maa Panoche Hills, California, USA	57, 3 pectorals (WELLES 1943, referred specimen); 59 (WELLES 1952)	/
Libonectes morgani (WELLES, 1949)	CARPENTER 1997, 1999	SMUSMP 69120, skull, cervicals (lost pectoral girdle and limbs)	Lower Tur Eagle Ford Group, Texas, USA	62	460
Elasmosaurus platyurus COPE, 1868	Carpenter 1997, 1999	ANSP 10081, skull fragments, partial vertebral column	Lower Cmp, Kansas, USA	72	/
Hydralmosaurus serpentinus (COPE, 1877)	WELLES 1943, STORRS 1999, CARPENTER 1999	AMNH 1495 partial skeleton; holotype of S. browni, skull, vertebrae, partial pectoral girdle, fore limb; AMNH 5835, patial skeleton	Cmp Pierre Shale, Nebraska, Wyoming, USA	63 (referred specimen)	400 (referred specimen)
Hydrotherosaurus alexandrae WELLES, 1943		UCMP 33912, supcomplete, skeleton	Maa Moreno Fm., California, USA	60, 2 pectorals	330
Morenosaurus stocki WELLES, 1943		CIT 2802, partial skeleton; referred juvenile CIT 2749, partial skull, neck, fore limb	Maa Panoche Hill, California, USA	46 (referred specimen)	/
Styxosaurus snowii (WILLISTION, 1890)	STORRS 1999 CARPENTER 1999	KUVP 1301, skull, cervicals, serveral referred specimens, including holotype of a *pembertoni*	Cmp Kansas, South Dakota, USA	62	480
Terminonatator ponteixensis SATO, 2003		RSM P2414.1, skull, partial post cranium	Upper Cmp, Saskatchewan Canada	(52 preserved)	270
Thalassomedon haningtoni WELLES, 1943	CARPENTER 1999	DMNH 1588, subcomplete skeleton; referred skull UNSM 50132, partial skeleton FMNH 12009	Lower Cen, Colorado, USA	62	510
Tuarangisaurus keyesi WIFFEN & MOISLEY, 1986	CARPENTER 1999	NZGS CD425 & 426,skull, cervicals; 3 referred partial juveniles	Cmp-Maa New Zealand	/	370

radius and ulna clearly differs from the situation characteristic of *Hydralmosaurus* (WELLES 1943, CARPENTER 1999).

The neural arch of the axis of SMNK-PAL 3978 is caudally directed, as in *Libonectes*, *Styxosaurus* and *Elasmosaurus*, rather than rising dorsally (CARPENTER 1999); the postzygapophysis of the axis extends further caudally than the caudal articular face of the axis, overhanging the centrum of C3, a condition also known in *Libonectes* but not in *Styxosaurus*, *Thalassomedon* or *Elasmosaurus* (CARPENTER 1997, 1999). The atlas/axis of *Hydrotherosaurus* appears to be similar in proportions to that of *Elasmosaurus* (WELLES 1943, CARPENTER 1999). In contrast to *Libonectes morgani*, whose axis neural arch is about half the height of its axis centrum, the axis neural arch of SMNK-PAL 3978 is about 1.5 time higher than its axis centrum. The nares of SMNK-PAL 3978 are situated dorsal to the largest maxillary teeth (numbers 4–5), similar to *Libonectes morgani* (where the largest teeth are number 3–4), while in *Styxosaurus* the nares are situated caudal to the largest maxillary teeth (WELLES & BUMP 1949, CARPENTER 1999). In *Thalassomedon* the nares are circular in outline and situated above maxillary teeth 3-5; the rostral-most teeth appear not to be procumbent (CARPENTER 1999).

Callawayasaurus colombiensis (WELLES, 1962), from the Aptian of Colombia, has 56 preserved cervicals (CARPENTER 1999). Its nares are situated above maxillary teeth 3–5; its skull is more brevirostrine than that of SMNK-PAL 3978 (WELLES 1962: figs 3, 4). The atlas/axis complex of *Callawayasaurus* is unknown.

Aphrosaurus furlongi WELLES, 1943 possesses 57 cervicals, plus 3 pectorals based on a referred juvenile specimen (WELLES 1943; the same author gives 59 cervicals plus 3 pectorals in his 1952 diagnosis). The antebrachial space is reduced in *Aphrosaurus furlongi* WELLES, 1943, as the radius has an almost straight caudal margin and the ulna an almost straight cranial one. The carpals of this taxon are said to be very thick, and the humerus appears narrow distally (WELLES 1943). This taxon is poorly defined; in any case, SMNK-PAL 3978 shares none of these features with it.

The (adult) holotype of *Terminonatator* SATO, 2003 comprises a poorly preserved skull and partial postcranium. Its diagnosis is somewhat puzzling in emphasising nine premaxillary teeth (including a central one that could result from abnormal growth, if not merely from lateral crushing) and a pointed, triangular coronoid process (which is invisible due to poor preservation in most other elasmosaurs known from otherwise adequate material). SMNK-PAL 3978 differs from the holotype and only known specimen of the taxon in its limb anatomy and most likely in lacking the craniolateral process of the pubis that is so conspicuous in *Terminonatator* (SATO 2003).

Tuarangisaurus WIFFEN & MOISLEY, 1986 possesses a brevirostrine skull (beak index 34, *versus* about 40 in SMNK-PAL 3978), with a wider maxillary rostrum than SMNK-PAL 3978; the nares are situated level with maxillary teeth 2–3 (WIFFEN & MOISLEY 1986: figs 1-3, CARPENTER 1999: fig. 14). The mandibular rostrum extends until between the second and third dentary teeth (WIFFEN & MOISLEY 1986, LONG 1998). Only about half the length of the axis postzygapophysis projects caudally over centrum 3 (WIFFEN & MOISLEY 1986: fig. 4).

It appears therefore that SMNK-PAL 3978 shares the diagnostic features of none of the Late Cretaceous elasmosaurid genera currently considered as valid (WELLES 1962, WIFFEN & MOISLEY 1986, BARDET et al. 1999, CARPENTER 1999, STORRS 1999, GASPARINI et al. 2003, SATO 2003). However, I consider it likely that the impossibility of referring this specimen to any hitherto described genus is most likely rooted in the inadequacy of many holotypes or referred specimens and their description and illustration, and, as a consequence, of elasmosaur taxonomy in general. I therefore do not elect to create a new genus that would mainly be diagnosed by features unknown in other taxa. Based on similar stratigraphical occurrence, SMNK-PAL 3978 is referred to the Turonian genus *Libonectes* CARPENTER, 1997 and the features unique to SMNK-PAL 3978 are arbitrarily given specific import to acknowledge the differences observed between the type of *Libonectes*, *L. morgani* (WELLES, 1949), and SMNK-PAL 3978. These are listed in the diagnosis.

Bone lesions

The affected bones are not adjacent (Table 1) and in the clearest instances they are neither distorted (the original outline being preserved; see Material, Fig. 7) nor displaced. It is highly unlikely that diagenesis caused such preservation in these bones. In contrast, several other bones clearly show signs of diagenetic distortion in the presumably affected areas (e.g., the right humerus and caudal-most cervical vertebrae: Fig. 8 and 7, respectively). The lesions are here interpreted as resulting from a pathology inducing a decrease in bone density. Provided this pathology affected the mineral frame of the bone (osteoid), the natural cast would then represent remains of the non-mineral fraction of the bone. Due to reduced mineral frame, the affected areas of the bones would have been 'soft' *in vivo*; collapse of the humerus, for instance, at the level of the affected area is explained by the resulting softening of the bone (ROTHSCHILD & MARTIN 1993). Pathologies inducing such a multilocular decrease in bone density without abnormal bone growth include osteoporosis and osteomalacia, and metabolic or hormonal diseases; disuse or immobilisation also result in reduction of bone density but appear unlikely in the case and location of the lesions observed in SMNK-PAL 3978 (cf. ROTHSCHILD & MARTIN 1993). Avascular necrosis, maybe resulting from decompression syndrome, could also be invoked, although the lesions in SMNK-PAL 3978 do not appear localised in the areas usually affected (subarticular portions of femur and humerus, ROTHSCHILD & MARTIN 1987, 1993, ROTHSCHILD & STORRS 2003). ROTHSCHILD & STORRS (2003) did diagnose decompression syndrome in plesiosaurs, but their systematic examination yielded no affected vertebrae while SMNK-PAL 3978 exhibits numerous affected cervical vertebrae (Table 1). According to these authors, the vertebrae were possibly highly vascularised as an evolutionary response to the risk of decompression syndrome. Proper diagnosis of the pathology in SMNK-PAL 3978 requires systematic examination of the internal structure of the affected areas, at least with X-rays (ROTHSCHILD & MARTIN 1993), which is not currently possible, as the specimen is on exhibition.

A different type of lesion is visible on some bones of the forelimb (Fig. 8). On the dorsal surface of the left humerus, a scratch mark terminated by a subcircular depression surrounded by a wider area where the bone appears pressed-in is present in the middle portion of the shaft. A larger, subcircular, depressed area filled with resin at the broken edge of the shaft possibly also represents a bite mark; the ulna shows a similar mark in its middle. The dorsal surface of the radius exhibits at least five possible circular, smaller bite marks.

Elasmosaur dentition, preliminary remarks

Elasmosaurids, together with the other long-necked, short-headed plesiosaurs of debated affinities, cryptoclidids and plesiosaurids (O'KEEFE 2001, GASPARINI et al. 2003, O'KEEFE & WAHL 2003), represent one of the few groups of tetrapods whose caudal-most tooth crowns are not lower than the rostral ones. Lowering of the caudal tooth crowns is a well-justified phenomenon on a biomechanical ground (e.g. GREAVES 1983, 1995). The caudal part of the tooth row encounters the highest forces during occlusion; more massive teeth in this part of the row better resist the stress. Being located closer to the pivot, the path traversed by their apex during the occluding phase is shorter, hence the caudal-most teeth are lower. MASSARE (1987) attributed the form of elasmosaur teeth a piercing (of fish) function. If that is arguable for the rostral-most teeth, it is certainly not the case for the caudal ones. Interaction of the caudal-most dentary teeth of SMNK-PAL 3978 (and most elasmosaurs) with even low caudal maxillary teeth in order to pierce a prey item would require such a gape (see e.g. Fig. 1, Table 3) that it appears impossible: if during the movement (provided it is allowed by the occipital joint) the skull is considered as the mobile element, the squamosal would be brought into contact with the axis neural arch. This would mean squeezing the supraspinsal ligament and local epaxial and depressor musculature (e.g. FREY 1988). If the skull is considered immobile during occlusion, and only the mandible moves, the movement (if allowed by the mandibular articulation) would bring the retoarticular process to collide with the suspensorium. The caudal portion of the tooth row cannot be considered a prey-piercing device, and still large caudal teeth are retained throughout the whole elasmosaur history. If the function of these teeth was not related to a vertical movement of the jaws, then one has to consider a function aligned with a horizontal movement – of the water flow: it is here preliminarily suggested that the elasmosaur tooth apparatus would constitute better a sieving device. COLLIN & JANIS (1997) argued that suspension feeding is most likely absent in fossil marine reptiles. Although the head of elasmosaurs is not large compared to their body (as would be required for suspension feeding: COLLIN & JANIS 1997), the mandible is consistently ogival in ventral aspect and tall in lateral aspect, which leaves space and attachment areas for a well-developed hyomandibular musculature and gular pouch. The absence of a bony secondary palate in plesiosaurs stands in contradiction to the hypothesis of suspension feeding; however COLLIN & JANIS (1997) recognise that a soft tissue equivalent can develop. The existence of such a device was indeed suggested for pliosaurs (MCHENRY pers. comm.). Some fossil evidence hint at an inflexible neck in plesiosaurs, at least in its cranial-most part (BUCHY et al. 2005), but still the length of the neck stands in contradiction to biomechanical requirements of a suspension feeder as analysed by COLLIN & JANIS (1997).

One hypothesis never explored to account for elasmosaurs' peculiar anatomy is sediment sieving for epi- or endobionts. Elasmosaurs evolved during highest transgression phases, when large, shallow, soft substrate areas became available for marine reptiles (e.g. SMITH et al. 1994; BARDET 1995; NOÈ et al. in prep.). Under this hypothesis the chin of SMNK-PAL 3978 forms a convenient plough. The intensive pitting of the premaxillary surface of elasmosaurs (e.g. WELLES 1962, WIFFEN & MOISLEY 1986, BARDET et al. 1999) could have housed exits for sensory terminations of the fifth cranial nerve, functionally analogous to Recent walruses' sensory bristles (RIDGWAY & HARRISON 1987). Although absent in SMNK-PAL 3978—at least in its present condition—gastroliths are regularly encountered within elasmosaurs' abdominal area (for a review see CICIMURRI & EVERHART 2001) and would be essential to access digestible parts of invertebrates. Finally, this does not contradict occasional capture of fish when available, but it would better explain the rarity of such identifiable gastric contents (CICIMURRI & EVERHART 2001).

Acknowledgements

Thanks are due to E. 'D.' FREY (SMNK) and R. SCHOCH (SMNS) for access to specimens in their care; and to E. 'D.' FREY also for comments upon the manuscript; to C. IFRIM (University of Karlsruhe) for ammonite determination; to N. BARDET (Paris), M. EVERHART (Hays), L. NOÈ (Cambridge) for discussion and literature; to K.T. SMITH (Yale University) who improved the present text by correcting the language and making valuable comments.

References

BARDET, N. (1995): Évolution et extinction des reptiles marins au cours du Mésozoïque. – Palaeovertebrata, **24** (3-4): 177-283.

BARDET, N., GODEFROIT, P. & SCIAU, J. (1999): A new elasmosaurid plesiosaur from the Lower Jurassic of Southern France. – Palaeontology, **42**: 927-952.

BARDET, N., PEREDA SUBERBIOLA, X., JALIL, N.-E. & LAROCHÈNE S. M. (2000): Marine reptiles from the early Late Cretaceous of the Goulmima region, Morocco. – 5th European Workshop on Vertebrate Palaeontology, Karlsruhe (Germany), 27 June - 01 July 2000, Abstract Book.

BARDET, N., PEREDA SUBERBIOLA, X. & JALIL, N.-E. (2003a): A new polycotylid plesiosaur from the Late Cretaceous (Turonian) of Morocco. – C. R. Palevol, **2**: 307-315.

BARDET, N., PEREDA SUBERBIOLA, X. & JALIL, N.-E. (2003b): A new mosasauroid (Squamata) from the Late Cretaceous (Turonian) of Morocco. – C. R. Palevol, **2**: 607-616.

BLAINVILLE, H. D. de (1835): Description de quelques espèces de reptiles de la Californie, précédée de l'analyse d'un système général d'Erpetologie et d'Amphibiologie. – Nouv. Ann. Mus. Nat. Hist. nat., Paris, **3** (4): 233-296.

BROWN, D. S. (1981): The English Upper Jurassic Plesiosauroidea (Reptilia) and a review of the phylogeny and classification of the Plesiosauria. – Bull. Br. Mus. (Nat. Hist.), Geol., **35** (4): 253-347.

BROWN, D. S. (1993): A taxonomic reappraisal of the families Elasmosauridae and Cryptoclididae (Reptilia: Plesiosauroidea). – Revue de Paléobiologie, Vol. spéc., **7**: 9-16.

BUCHY, M.-C., MÉTAYER, F. & FREY, E. (2005): Osteology of *Manemergus anguirostris* n. gen. et sp., a new plesiosaur (Reptilia, Sauropterygia) from the Upper Cretaceous of Morocco. – Palaeontographica, A **272**: 97-120.

CALDWELL, M. W. (1997): Limb osteology and ossification patterns in *Cryptoclidus* (Reptilia: Plesiosauroidea) with a review of Sauropterygian limbs. – J. Vert. Pal., **17** (2): 295-307

CARPENTER, K. (1997): Comparative cranial anatomy of two North American Cretaceous plesiosaurs. – In: CALLAWAY J. M. & NICHOLLS E. L. (Eds): Ancient Marine Reptiles: 191-216; San Diego (Academic Press).

CARPENTER, K. (1999): Revision of North American elasmosaurs from the Cretaceous of the western interior. – Paludicola, **2** (2): 148-173.

CAVIN, L. (1995): *Goulmimichthys arambourgi* n.g., n.sp., un Pachyrhizodontidae (Actinoptrygii, Teleostei) d'une nouvelle localité à nodules fossilifères du Turonien inférieur marocain. – C. R. Acad. Sci. Paris, **321**, II a: 1049-1054.

CAVIN, L. (1997): Nouveaux Teleostei du gisement du Turonien inférieur de Goulmima (Maroc). – C. R. Acad. Sci. Paris, Sci. Terre et planètes, **325**: 719-724.

CAVIN, L. (1999): Occurrence of a juvenile teleost, *Enchodus* sp., in a fish gut content from the Upper Cretaceous of Goulmima, Morocco. – Palaeontology Sp. Pap., **60**: 57-72.

CAVIN, L. (2001): Osteology and phylogenetic relationships of the teleost *Goulmimichthys arambourgi* Cavin, 1995, from the Upper Cretaceous of Goulmima, Morocco. – Eclog. geol. Helvetica, **94**: 509-535.

CAVIN, L., BOUDAD, L., DUFFAUD, S., KABIRI, L., LE LŒUFF, J., ROUGET, I. & TONG, H. (2001): L'évolution paléoenvironnementale des faunes de poissons du Crétacé supérieur du bassin du Tafilalt et des régions avoisinantes (Sud-Est du Maroc): implications paléobiogéographiques. – C. R. Acad. Sci. Paris, Sci. Terre et planètes, **333**: 677-683.

Chancellor, G. R., Kennedy, W. J. & Hancock, J. M. (1994): Turonian ammonite faunas from central Tunisia. – Palaeontology Sp. Pap., **50**: 1-118.

Cicimurri, D. J. & Everhart, M. J. (2001): An elasmosaur with stomach contents and gastroliths from the Pierre Shale (Late Cretaceous) of Kansas. – Trans. Kansas Acad. Sci., **104** (3/4): 129-143.

Collin, R. & Janis, C. M. (1997): Morphological constraints on tetrapod feeding mechanisms: why where there no suspension-feeding marine reptiles? – In: Callaway J. M. & Nicholls E. L. (Eds): Ancient Marine Reptiles: 451-466; San Diego (Academic Press).

Cope, E. D. (1868): On a new large enaliosaur. – Proc. Acad. Nat. Sci. Philadelphia, **20**: 92-93.

Cope, E. D. (1869): Synopsis of the extinct Batrachia, Reptilia and Aves of North America. – Trans. Amer. Phil. Soc., n. s., **14**: 1-252.

Everhart, M. J. (in press): Bite marks on an elasmosaur (Sauropterygia; Plesiosauria) paddle from the Niobrara Chalk (Upper Cretaceous) as probable evidence of feeding by the lamniform shark, *Cretoxyrhina mantelli*. – PalArch.

Ferrandini, M., Philip, J., Babinot, J.-F., Ferrandini, J. & Tronchetti, G. (1985): La plate-forme carbonatée du Cénomanien-Turonien de la région d'Erfoud-Errachidia (Sud-Est marocain): stratigraphie et paléoenvironnements. – Bull. Soc. géol. France, sér; 8, **I**: 559-564.

Frey, E. (1988): Anatomie des Körperstammes von *Alligator mississipiensis* Daudin. – Stuttgarter Beitr. Naturk., Ser. A, **42**: 1-106.

Gasparini, Z., Bardet, N., Martin, J. E. & Fernandez, M. (2003): The elasmosaurid plesiosaur *Aristonectes* Cabrera from the latest Cretaceous of South America and Antarctica. – J. Vert. Pal., **23**(1): 89-103.

Greaves, W. S. (1983): A functional analysis of carnassial biting. – Biol. J. Linn. Soc., **20**: 353-363.

Greaves, W. S. (1995): Functional predictions from theoretical models of the skull and jaws in reptiles and mammals. – In*:* Thomason, J. J. (Ed.): Functional morphology in vertebrate paleontology: 99-115; Cambridge Cambridge (University Press).

Kossmat, F. (1897): Untersuchungen über die Südindische Kreideformation. Zweiter Teil. – Beitr. Paläont. Österreich-Ungarns u. Orient, **11**: 1-46 (108-153), plates 1-8 (12-19).

Lazo, D. G. & Chichowolski, M. (2003): First plesiosaur remains from the lower Cretaceous of the Neuquen Basin, Argentina. – J. Paleont., **77** (4): 784-789.

Long, J. A. (1998): Dinosaurs of Australia and New Zealand and other animals of the Mesozoic Era. – 188 pp.; Sydney (University of New South Wales Press).

Massare, J. A. (1987): Tooth morphology and prey preference of Mesozoic marine reptiles. – J. Vert. Pal., **7** (2): 121-137.

Nickel, R., Schummer, A. & Seiferle, E. (2004): Lehrbuch der Anatomie der Haustiere, Bd. 1 Bewegungsapparat. – 8th Edition, 626 pp.; Stuttgart (Parey Verlag).

O'Keefe, F. R. (2001): A cladistic analysis and taxonomic revision of the Plesiosauria (Reptilia: Sauropterygia). – Acta Zool. Fennica, **213**: 1-63.

O'Keefe, F. R. & Wahl, W. (2003): Current taxonomic status of the plesiosaur *Pantosaurus striatus* from the Upper Jurassic Sundance Formation, Wyoming. – Paludicola, **4**(2): 37-47

Owen, R. (1860): On the orders of fossil and recent Reptilia, and their distribution in time. – Rep. Brit. Ass. Adv. Sci., 1859, **29**: 153-166.

Persson, P. O. (1963): A revision of the classification of the Plesiosauria, with a synopsis of the stratigraphical and geographical distribution of the group. – Lunds Universitets Arsskrift, N.F. Avd. 2, **59**: 1-59.

Ridgway, S. H. & Harrison, R. J. (1987): Handbook of marine mammals. 5 volumes; San Diego (Academic Press).

Romer, A. S. (1956): Osteology of the Reptiles. 772 pp.; Chicago and London (University of Chicago Press).

Rothschild, B. M. & Martin, L. D. (1987): Avascular necrosis: occurrence in diving Cretaceous mosasaurs. – Science, **236**: 75-77

Rothschild, B. M. & Martin, L. D. (1993): Paleopathology: disease in the fossil record. – 386 pp.; Boca Raton (CRC Press).

Rothschild, B. M. & Storrs, G. W. (2003): Decompression syndrome in plesiosaurs (Sauropterygia: Reptilia). – J. Vert. Pal., **23**(2): 324-328.

Rouvière, H. & Delmas, A. (1985): Anatomie humaine. – 12th Edition, t. 2, Masson, Paris.

Sato, T. (2003): *Terminonatator ponteixensis*, a new elasmosaur (Reptilia; Sauropterygia) from the Upper Cretaceous of Saskatchewan. – J. Vert. Pal., **23** (1): 89-103.

Shuler, E. W. (1950): A new elasmosaur from the Eagle Ford Shale of Texas. – Southern Methodist Univ., Fondren Science Series, **1** (2): 1-30.

Smith, A. G., Smith, D. G. & Funnel, B. M. (1994): Atlas of Mesozoic and Cenozoic coastlines. – 99 pp.; Cambridge (Cambridge University Press).

Storrs, G. W. (1997): Morphological and taxonomic clarification of the genus *Plesiosaurus*. – In: Callaway, J. M. & Nicholls, E. L. (Eds.): Ancient Marine Reptiles: 145-190; San Diego (Academic Press).

Storrs, G. W. (1999): An examination of Plesiosauria (Diapsida: Sauropterygia) from the Niobrara Chalk (Upper Cretaceous) of central North America. – Univ. Kansas Paleont. Contr., **11**: 1-15.

Taylor, M. (1997): Before the dinosaur: the historical significance of the fossil marine reptiles. – In: Callaway J. M. & Nicholls E. L. (Eds): Ancient Marine Reptiles: XIX-XLVI; San Diego (Academic Press).

Welles, S. P. (1943): Elasmosaurid plesiosaurs with a description of new material from California and Colorado. – Mem. Univ. Calif., **13**(3): 125-215.

Welles, S. P. (1949): A new elasmosaur from the Eagle Ford Shale of Texas. – Fondren Sci. Ser., Southern Methodist Univ., **1**: 1-28.

WELLES, S. P. (1952): A review of the North American Cretaceous elasmosaurs. – Univ. Calif. Publs geol. Sci., **29**(3): 47-144.

WELLES, S. P. (1962): A new species of Elasmosaur from the Aptian of Colombia and a review of the Cretaceous plesiosaurs. – Univ. Calif. Publs Geol. Sci., **44**(1): 1-96.

WELLES, S. P. & BUMP, J. (1949): *Alzadasaurus pembertoni*, a new elasmosaur from the Upper Cretaceous of South Dakota. – J. Paleont., **23**: 521-535.

WERNER, C. & BARDET, N. (1996): New record of elasmosaurs (Reptilia, Plesiosauria) in the Maastichtian of the Western Desert of Egypt. – Berliner geowiss. Abh., **E18**: 335-341.

WIFFEN, J. & MOISLEY, W. L. (1986): Late Cretaceous reptiles (Families Elasmosauridae and Pliosauridae) from the Mangahouanga Stream, North Island, New Zealand. – N. Z. J. Geol. Geophys., **29**: 205-252.

WILLISTON, S. W. (1890): A new plesiosaur from the Niobrara Cretaceous of Kansas. – Trans. Kansas Acad. Sci., **12**: 174-178.

WILLISTON, S. W. (1906): North American plesiosaurs: *Elasmosaurus*, *Cimoliasaurus*, and *Polycotylus*. – Am. J. Sci., **21**: 221-236.

WILLISTON, S. W. (1925). Osteology of the reptiles. – 300 pp.; Cambridge, USA (Harvard University Press).

Plate **1**: SMNK-PAL 3978, *Libonectes atlasense* n. sp., holotyope; general view of the mounted specimen. Total length about 7.2 m.

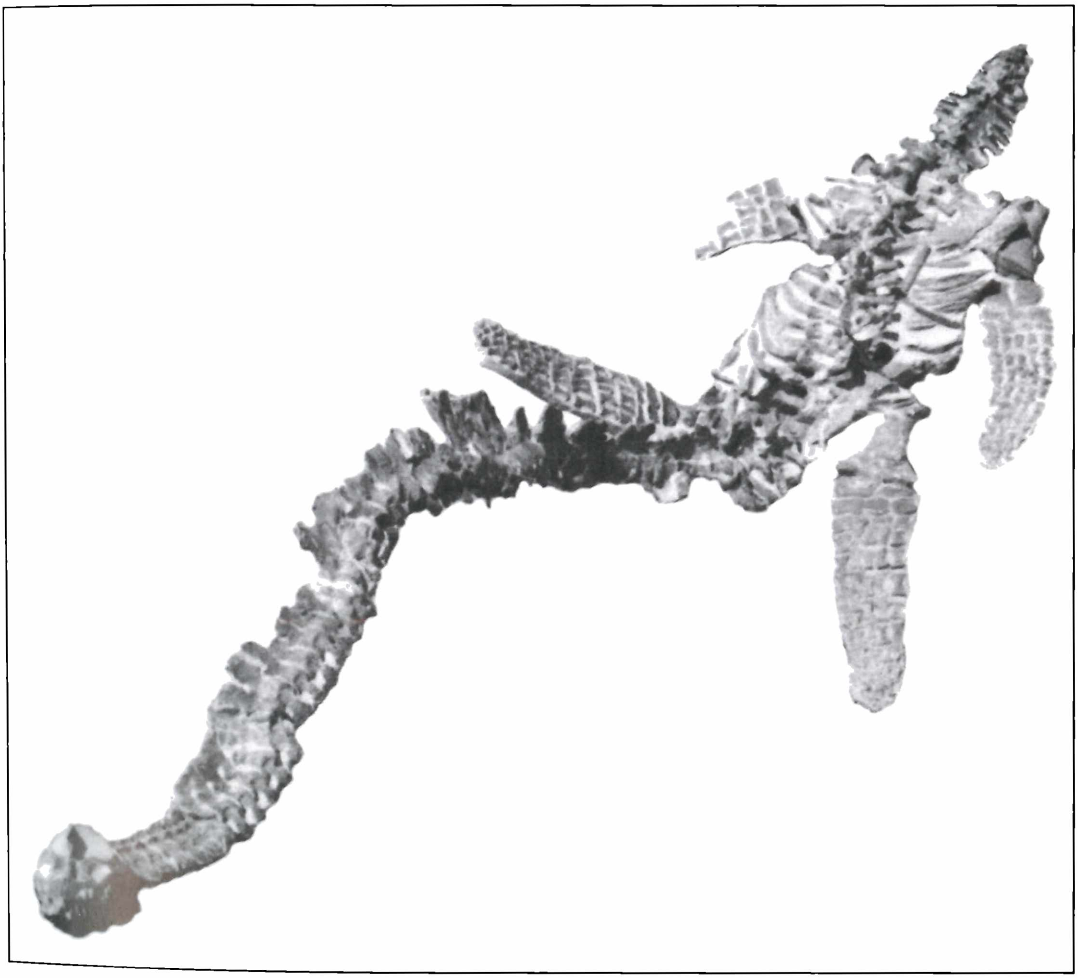

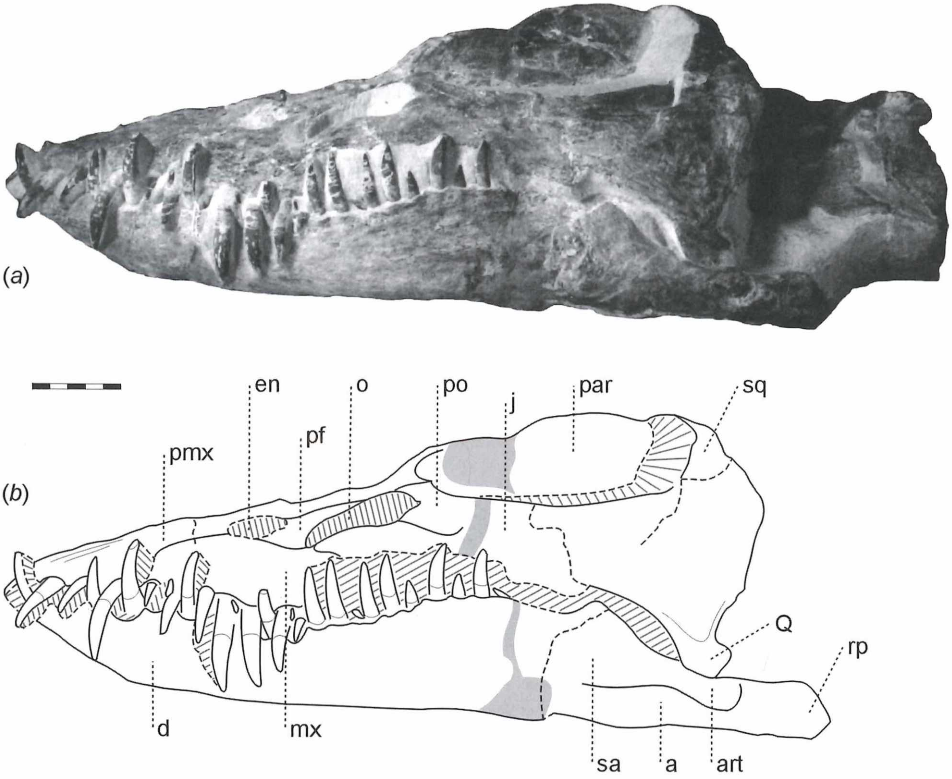

Figure 1: SMNK-PAL 3978, *Libonectes atlasense* n. sp., holotype; (*a*) skull in left lateral view; (*b*) interpretative line drawing. Abbreviations: a: angular; art: articular; d: dentary; en: naris; j: jugal; mx: maxilla; o: orbit; par: parietal; pmx: premaxilla; po: postorbital; pf: prefrontal; Q: quadrate; rp: retroarticular process; sa: surangular; sq: squamosal. Matrix is hatched. Shaded areas are reconstructed. Scale bar 50 mm.

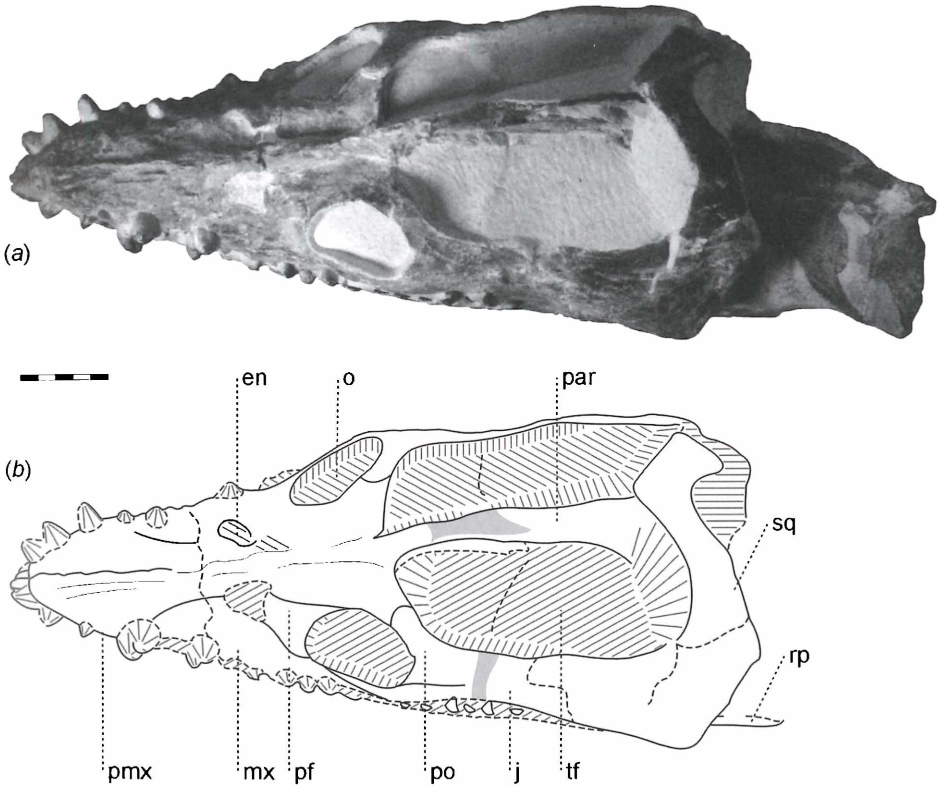

Figure 2: SMNK-PAL 3978, *Libonectes atlasense* n. sp., holotype; (*a*) skull in dorsal view; (*b*) interpretative line drawing. Abbreviations as in Figure 1, plus: tf: temporal fenestra. Matrix is hatched. Shaded areas are reconstructed. Scale bar 50 mm.

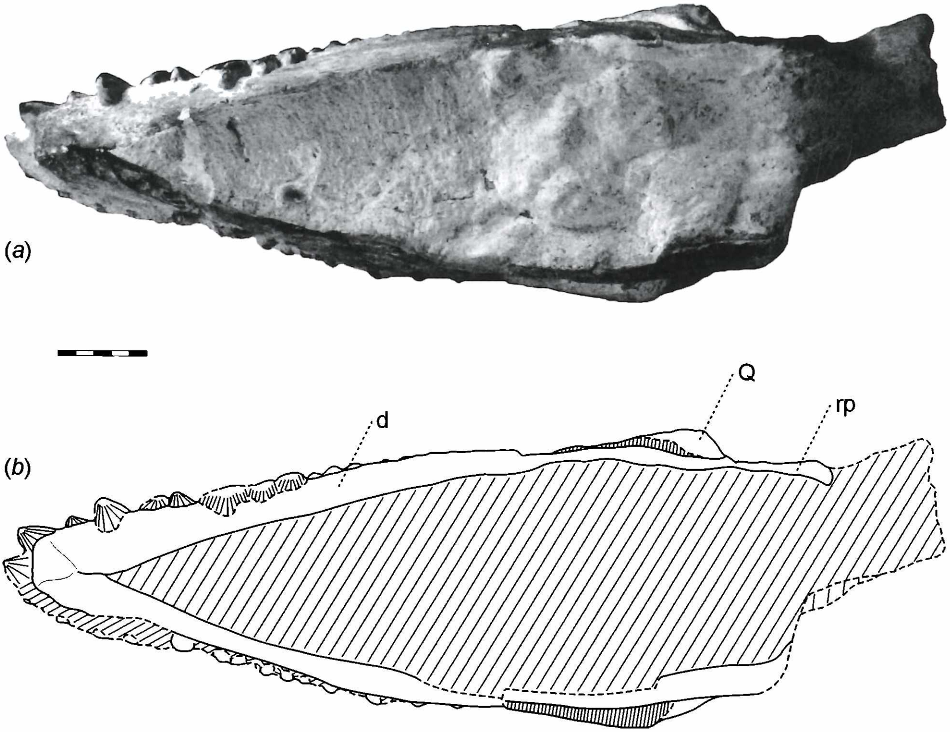

Figure 3: SMNK-PAL 3978, *Libonectes atlasense* n. sp., holotype; (*a*) skull in ventral view; (*b*) interpretative line drawing. Abbreviations as in Figure 1. Matrix is hatched. Shaded areas are reconstructed. Scale bar 50 mm.

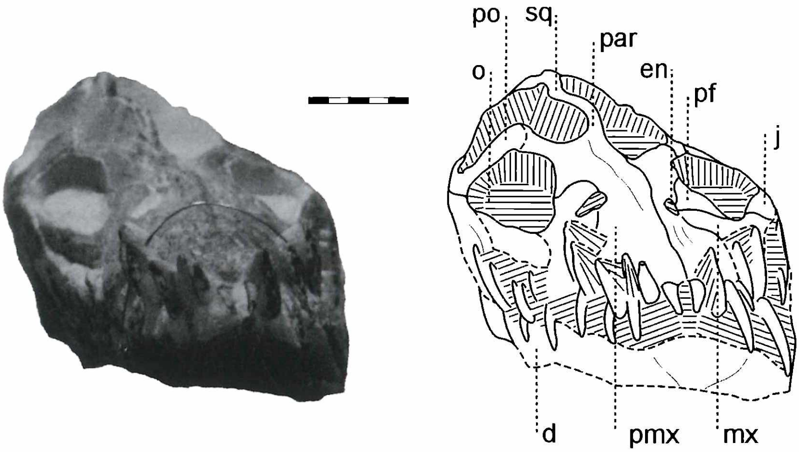

Figure 4: SMNK-PAL 3978, *Libonectes atlasense* n. sp., holotype; (*a*) skull in rostral view; (*b*) interpretative line drawing. Abbreviations as in Figure 1. Matrix is hatched. Shaded areas are reconstructed. Scale bar 50 mm.

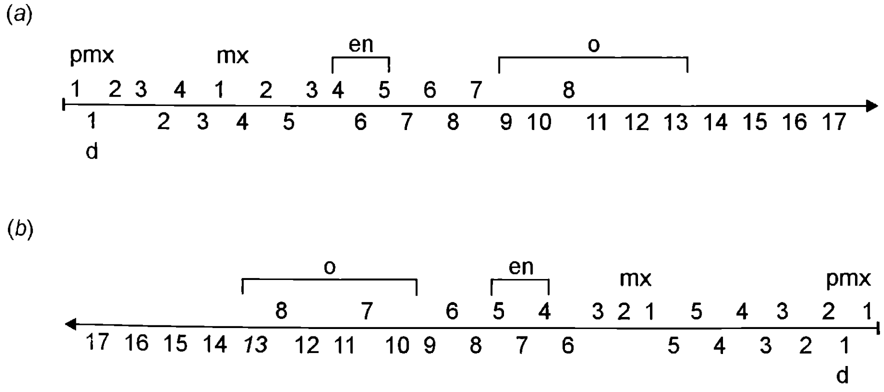

Figure 5: SMNK-PAL 3978, *Libonectes atlasense* n. sp., holotype; schematic illustration of the occlusion pattern. (*a*) left side, (*b*) right side. Abbreviations as in Figure 1. Not to scale.

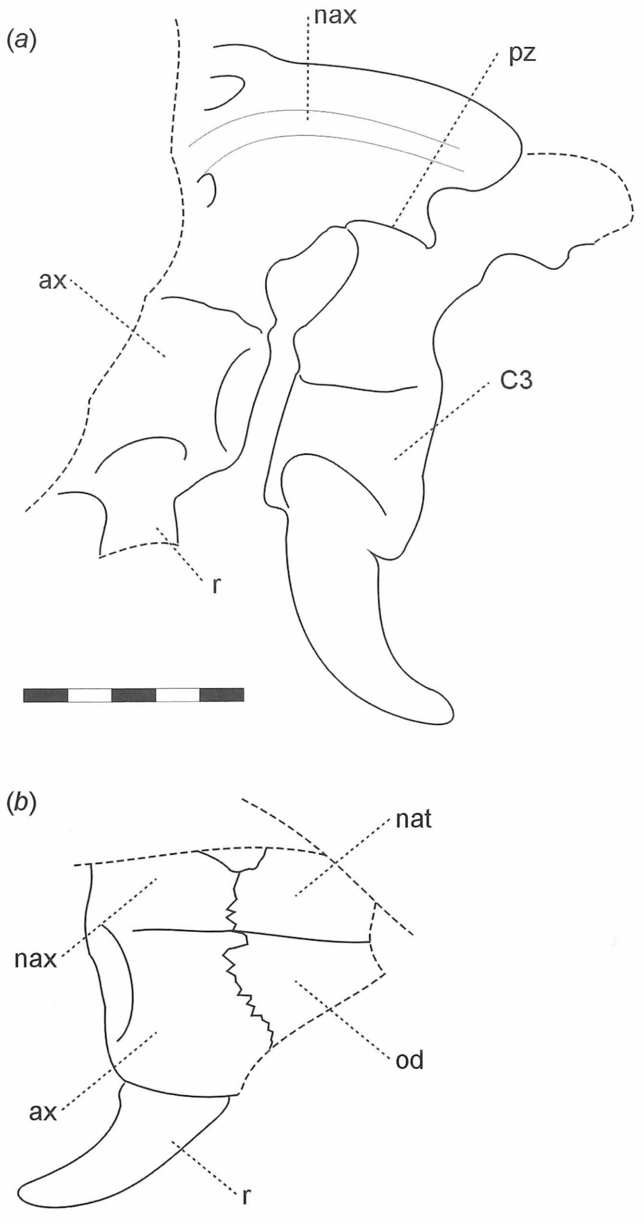

Figure 6: SMNK-PAL 3978, *Libonectes atlasense* n. sp., holotype; interpretative drawings of the atlas/axis complex (*a*) in left lateral view; (*b*) in right lateral view. Abbreviations: ax: axis; C3: third cervical vertebra; nax: axis neural arch; nat: atlas neural arch; od: odontoid; pz: atlas postzygapophysis; r: cervical rib. Scale bar 50 mm.

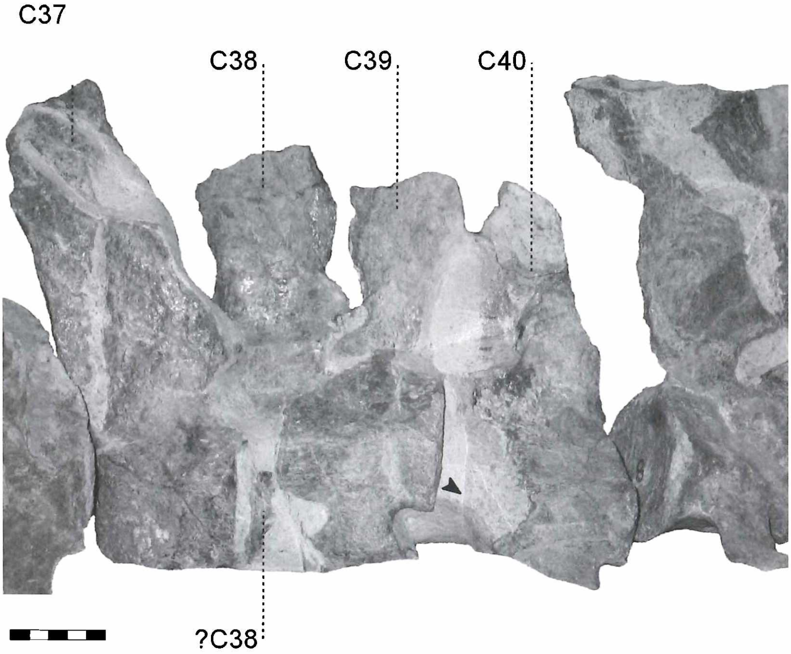

Figure 7· SMNK-PAL 3978, *Libonectes atlasense* n. sp., holotype; cervicals 37-41. Note vertebra C38 wedged between C37 and C39; arrow points at the cranial portion of C40 preserved as a natural cast, probably due to a pathology (see text). Scale bar 50 mm.

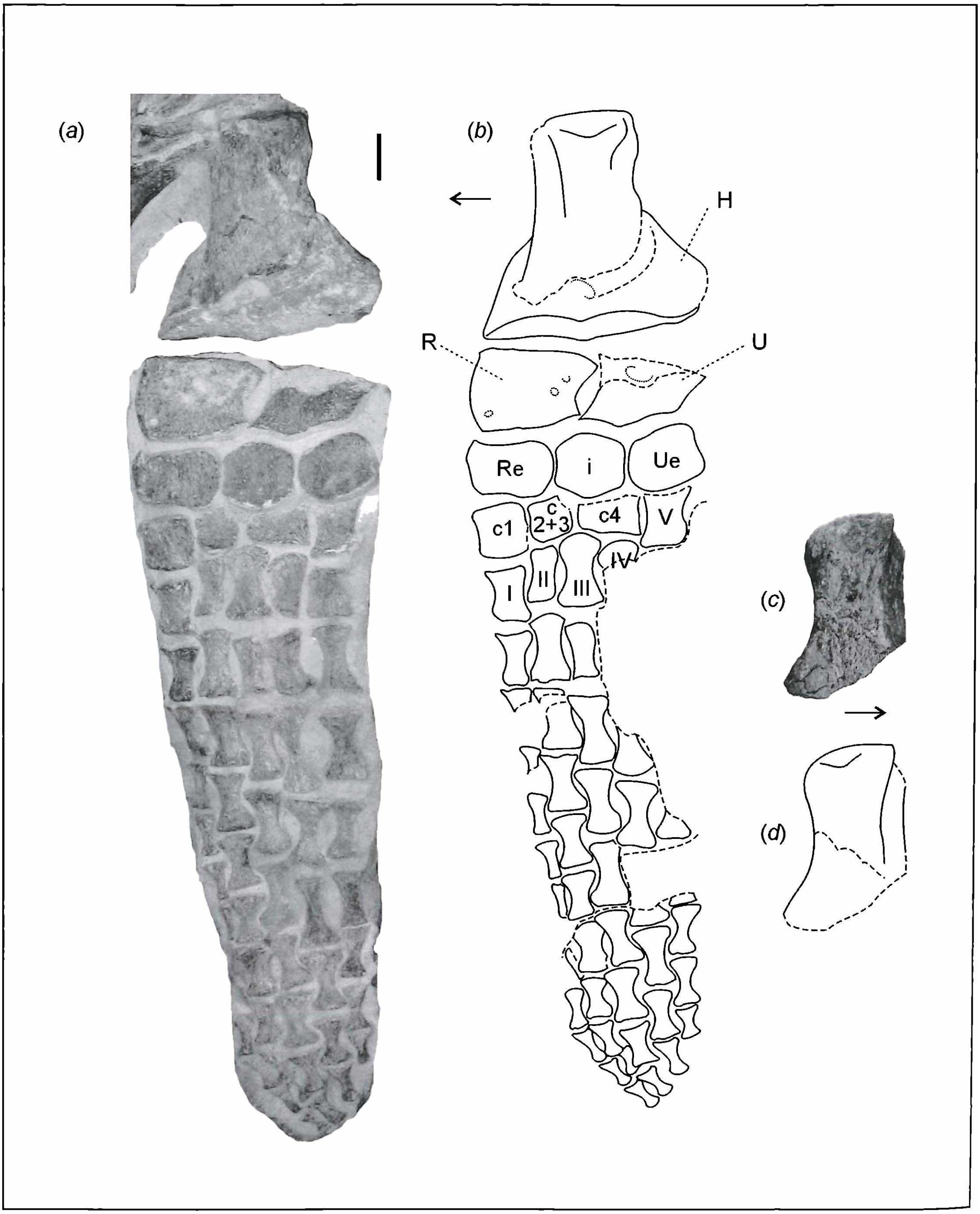

Figure 8: SMNK-PAL 3978, *Libonectes atlasense* n. sp., holotype; (*a*) left forelimb in dorsal view; (*b*) interpretative drawing; (*c*) right humerus in dorsal view; (*d*) interpretative drawing. Abbreviations: c1-4: distal carpals 1-4 (see text); H: humerus; i: intermedium or centrale (see text); R: radius; Re: radiale; U: ulna; Ue: ulnare; I-V: metacarpals I-V. Arrows point cranially. Dashed lines mark breaks or reconstructed margins. Dotted lines mark possible bite and scratch marks. Scale bar 50 mm.

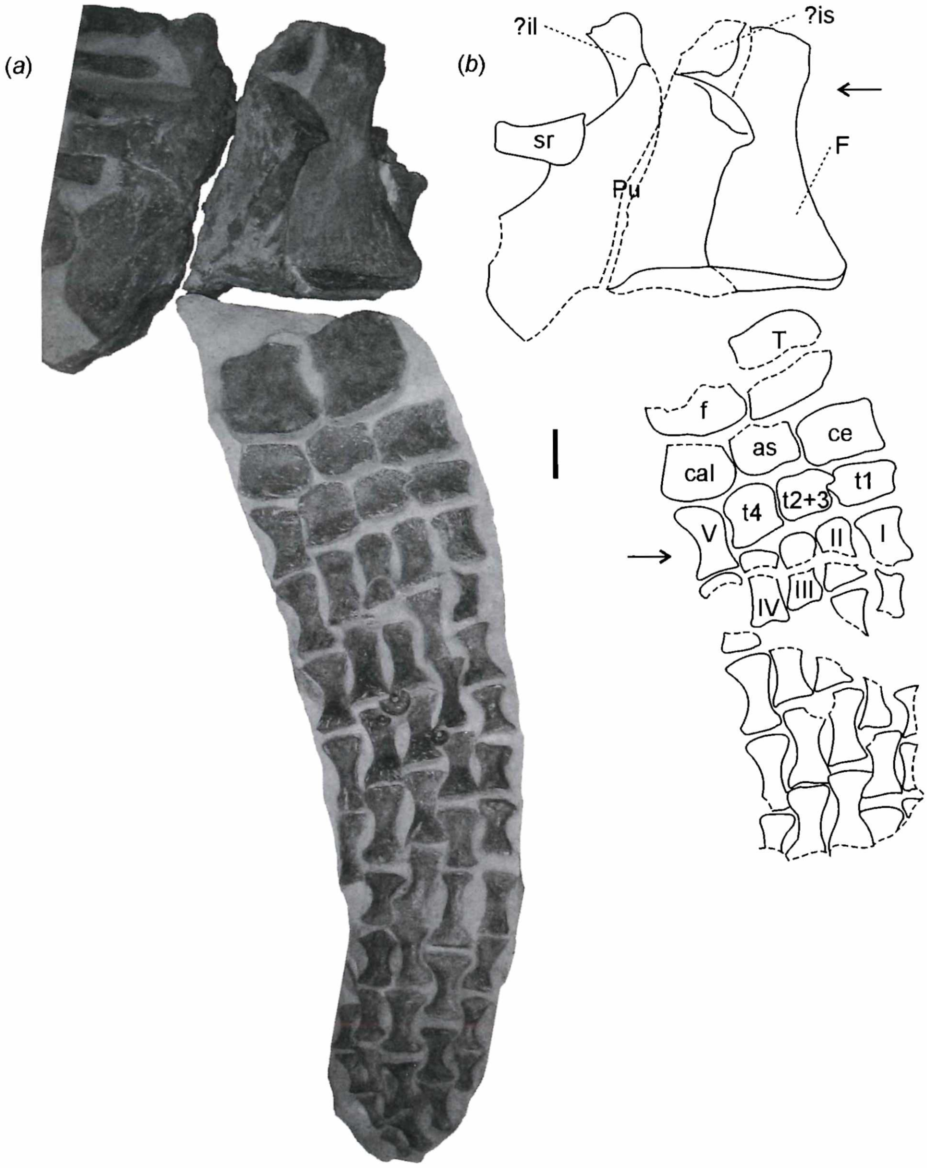

Figure 9: SMNK-PAL 3978, *Libonectes atlasense* n. sp., holotype; (*a*) left hindlimb as exhibited: the girdle and femur are visible in dorsal view while the rest of the limb is either the right one in dorsal view or the left one in ventral view (see text); (*b*) interpretative drawing. Abbreviations: as: astragalus; cal: calcaneum; ce: centrale; il: ilium; is: ischium; F: femur; f: fibula; Pu: pubis; sr: sacral rib; t1-4: distal tarsals 1-4 (see text); T: tibia; I-V: metatarsals I-V. Arrows for orientation of the limb elements point cranially. Dashed lines mark breaks or invisible margins. Scale bar 50 mm.

Figure 10: SMNS 81783, *Libonectes atlasense* n. sp., referred specimen in left dorsolateral view. Scale bar 50 mm.

Zeitschrift/Journal: Carolinea - Beiträge zur naturkundlichen Forschung in Südwestdeutschland

Jahr/Year: 2006

Band/Volume: 63

Autor(en)/Author(s): Buchy Marie-Céline

Artikel/Article: An Elasmosaur (Reptilia: Sauropterygia) from the Turanian (Upper Cretaceous) of Morocco 5-28